Stochastic treatment of perforation phenomenon induced by laminar-turbulent transition in a thin liquid sheet

Azuma T., Wakimoto T.

Osaka City University, Sugimoto 3-3-138, Sumiyoshi-ku, Osaka, 558 Japan

This paper describes the perforation and disintegration of a radially thinning liquid sheet, which is induced by laminar-turbulent transition. The perforation phenomenon is clarified by high-speed photography and by using an electric perforation sensor for detecting the passage of perforation. A stochastic relation between the void fraction, i.e. the time fraction that a reference point is within passing perforations, and the rate of occurrence of new perforation per unit area at upstream positions of the point is formulated. The radial distribution of the rate of occurrence of perforation is estimated from the void fraction measured at a series of downstream positions. This estimation reveals that innumerable perforations occur immediately after the transition at extremely high Reynolds number.

I. Introduction

The atomization of liquids is of primary importance in many industrial processes. The most susceptible flow form for the disintegration of liquid into drops is a thin sheet of liquid, since it has the highest surface energy and thus the great instability. However, because of the complexity of the phenomenon, the mechanism of the disintegration has not yet been completely clarified.

Two kinds of breakup mechanisms of the moving liquid sheet have been investigated theoretically and experimentally: the one is the growth of sinuous wave motion resulting in ligament formation [1]-[4] and the other is the occurrence of perforation in the liquid sheet [5][6]. However, no investigator pays attention to the breakup phenomenon directly induced by a sudden transition from laminar liquid sheet to turbulent one, which is attributable to the velocity distribution inside the liquid sheet.

The authors found out that sudden laminar-turbulent transition occurs in the radial liquid film flow on a disk when the Reynolds number exceeds a critical value [7][8]. They also found out that the transition occurs in a radially thinning liquid sheet, which is generated by the leaving of the radial liquid film on the disk from its peripheral edge into the atmosphere [9]-[11]. Expecting that the transition results in the liquid integration, the authors observed a series of processes of transition, perforation and disintegration into drops under a broad range of the Reynolds number [12].

In the present paper, perforation phenomenon appeared in the liquid sheet is clarified by photography and by using an electric perforation sensor for both detecting the passage of perforation and the obtaining the void fraction, i.e. the time fraction that the measuring point is within passing perforations. On the other hand, a stochastic relation between the void fraction at a reference point and the rate of occurrence of perforation at upstream positions of the point is formulated. Then, the radial distribution of the rate of occurrence of perforation is estimated

from the void fraction measured at a series of downstream positions. Thus, it is indicated that the transition results in the complete disintegration of the liquid sheet into drops.

2. Experimental description

Figure 1 shows the experimental apparatus. A cylindrical thin gap was formed between the lower end of a circular pipe and the flat top surface of a horizontally placed disk. When pressured tap water flows out from this gap, a radial liquid film flow is formed on the disk. Such a liquid film, in which the velocity distribution of laminar boundary layer is fully developed, flows from the edge of the disk into the still air so that a radial liquid sheet is formed. The inner diameter of the pipe was 25 mm and the disk diameter was 60 mm. The distance of the gap between the pipe end and the disk surface was maintained at 0.15 mm.

In order to obtain a stagnant pressure at the disk center, the static pressure inside the pipe at 650 mm upstream position from the pipe end was measured using a pressure transducer. The maximum stagnant pressure achievable in this apparatus was 800 kPa.

The processes of the perforation and disintegration of the liquid sheet were photographed by a steel camera under a strobe flush duration of 30 μs. The growth and travel of perforation were also observed by high-speed continuous photography, in which a drum streak camera was used with a high-speed strobe of a flash duration of 10 μs and a flash interval of 1 ms. In addition, the passage frequency of perforation and the void fraction at each radial position were measured by an electric perforation sensor, which was constructed by a 50 μm stainless-steel wire placed perpendicular to the liquid sheet.

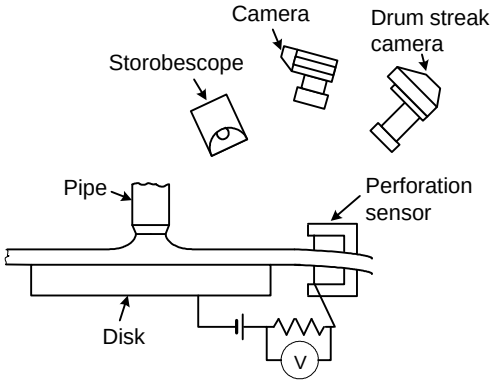

Fig. 1 Experimental apparatus

3. Experimental results

The flow condition through the gap is indicated by the discharge Reynolds number, Re_0, defined by $Re_0=Q/(CDH)^{1/2}$ ν, where Q is the volume flow rate, D is the inner diameter of the pipe, H is the gap distance, C is the discharge coefficient of the gap and ν is the kinematic viscosity. C is obtained by $C=Q/\pi DH(2p/\rho)^{1/2}$, where p is the stagnant pressure and ρ is the density. It has been confirmed that the velocity profile and the liquid film thickness of the laminar liquid film flow on the disk were in good agreement with Watson's analysis [7][13].

Table 1 Flow conditions of Photographs in the present paper

Fig. No.	p kPa	Q L/s	T ºC	Re_0 x10^{-3}	U_e m/s	h_e μm	Re_e	U_u m/s
2-a	200	0.146	16	86	15.8	79.8	1130	12.2
2-b	364	0.196	18	120	23.5	72.1	1580	18.2
2-c	497	0.228	19	143	28.6	68.8	1880	22.1
3	734	0.322	17	182	38.0	73.2	2580	29.4
4	358	0.224	16	124	24.7	78.4	1740	19.1

3.1 Perforation of liquid sheet

The flow conditions of photographs presented in the present paper are shown in Table 1, where T is the water temperature, U is the liquid surface velocity, h is the liquid film thickness and Re is the local Reynolds number defined by $Re=Uh/\nu$. The subscript e denotes the value at the edge of the disk. Values of U_e and h_e are calculated from Watson's analysis. U_u denotes the liquid-sheet velocity at a far downstream location where the velocity distribution is uniform. The value of U_u for the laminar liquid sheet can be obtained under conservations of mass and momentum, and $U_u=0.773U_e$ [9]. That this relation is also approximately applicable for the liquid sheet, in which the laminar-turbulent transition occurs, was confirmed by LDV measurement [11].

Figures 2 show perforation phenomena of the liquid sheet. The scale presented above each photo in Figs. 2 indicates the radial distance from the center of the disk. When $Re_0=8.6\text{x}10^4$, Fig. 2(b), a laminar-turbulent transition occurs at 4 to 5mm downstream of the disk edge, as indicated by arrow 'a'. When the transition occurs, the liquid sheet is covered with micro granular waves, which appeared white in the photograph due to the scattering of light ray on the liquid surface. Since these granular waves are converted to ripple waves of fairly large wavelength sufficiently downstream of the transition point, the liquid sheet is observed to be transparent until it fluctuates such as a flag motion at r=120 mm. A perforation appears in the liquid sheet before the flag wave motion (arrow 'b'). The occurrence of this perforation is seemingly attributable either to the granular waves in the transition region or to the ripple wave region further downstream of the transition point. On the other hand, many perforations are also observed in the flag wave (arrow 'c'). The number of perforation appeared in the liquid sheet increases with Re_0. In Fig. 2(b), the size of perforation at a smaller radial position is generally smaller than that of perforation at further downstream position because a perforation expands downstream. When the frequency of occurrence of perforation further increases with Re_0, the boundaries between adjacent perforations are deformed into liquid strands to form a net pattern. These liquid strands are cut to breaks up into many drops. In this case, no flag wave appears naturally. When $Re_0=1.43\text{x}10^5$, Fig. 2(c), a large number of perforations occurs owing to the intense turbulence just after the transition. However, the net structure of liquid strands is still observed clearly within a radius of 80 mm.

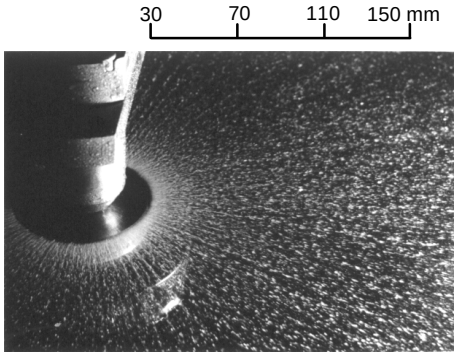

Fig. 3 Disintegration of radial liquid sheet due to transition. $Re_0=1.82\text{x}10^5$.

Figure 3 shows the characteristic feature of the liquid sheet under $Re_0=1.8\text{x}10^5$, in which the transition occurs at 3 to 4 mm downstream location from the disk edge. The frequency of

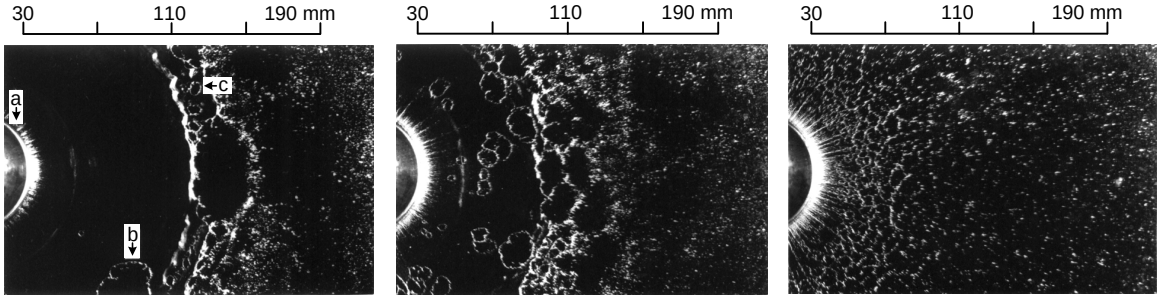

(a) $Re_0=8.6\text{x}10^4$ (b) $Re_0=1.20\text{x}10^5$ (c) $Re_0=1.43\text{x}10^5$

Fig. 2 Characteristic feature of radial liquid sheet

occurrence of perforation just after the transition point increases significantly. As a result, any perforation is not distinguished visually and the atomization of the liquid sheet seems to be realized at the moment of the transition.

3.2 Growth and travel of perforation

For a small puncture in an infinitely extended liquid sheet of uniform thickness, Fraser et al. [14] derived the rate of growth of a perforation under the balance of the surface tension force on the rim around the perforation and the inertial force of liquid accumulated at the rim. In the radial liquid sheet, a perforation occurred in the sheet continue to grow elliptically downstream because of the radial spreading of the flow. We now take account of the radial spreading of the flow and assume that a perforation travels with the same velocity of the liquid sheet. When a perforation occurred at $r=r_0$ travels to r, the shorter length (radial length), d_r, and longer length (circumferential length), d_c, of the elliptic perforation at a radius of r are calculated by

$$d_r(r) = \frac{2}{U_u}\int_{r_0}^{r}\sqrt{\frac{2s}{r\,h(r)}}\,dr \tag{1}$$

$$d_c(r) = d_r(r) + 2\int_{r_0}^{r}\frac{d_r(r)}{\sqrt{d_r(r)^2 + 4r^2}}\,dr \tag{2}$$

where $h(r)=Q/2\pi r U_u$ is the liquid thickness.
In order to confirm the validity of Eqs. (1) and (2), we took high-speed continuous photographs of a perforated liquid sheet, the flow condition of which is listed in Table 1. These consecutive photographs are shown in Figs. 4. The time interval between each photo is 1 ms and the scale presented above each photo indicates the radial distance from the center of the disk.
A perforation observed at r=45 mm and indicated by arrow ‘a’ in Fig. 4(a) grows elliptically and travels downstream with time as indicated by arrows ‘a’ in Figs. 4(b) and (c), and is about to coalesce with another perforation indicated by arrows ‘b’ in Fig. 4(b) and (c). The traveling velocity of the center of the perforation of ‘a’ in Figs. 4(a) to (c) is about 20m/s and this value is almost the same as U_u (=19.1 m/s) shown in Table 1. Hence, it is found that the center of the perforation travels with the velocity of the liquid sheet.
Figure 5 shows the radial location of center and the size of perforation with progressing time. In this figure, experimental data is obtained from high-speed photographs, and data indicated by circle correspond with the perforations indicated by arrows ‘a’ in Figs. 4. In addition, white and black marks indicate the radial and circumferential length of elliptic perforation,

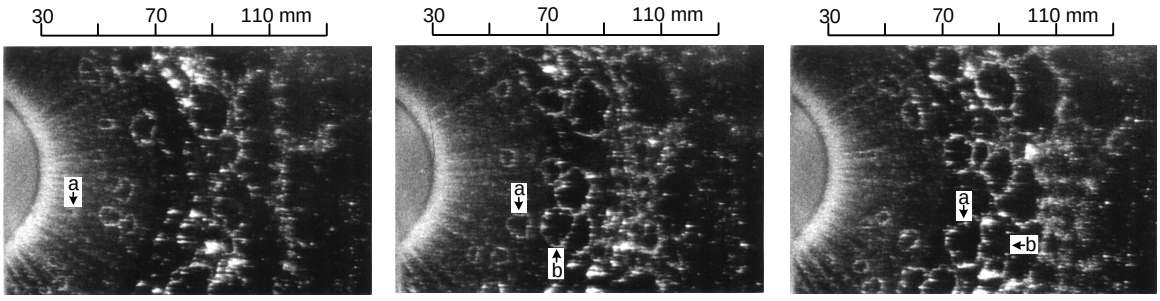

(a) (b) (c)

Fig. 4 High-speed photography of growth and travel of perforation. Frame interval is 1 ms.

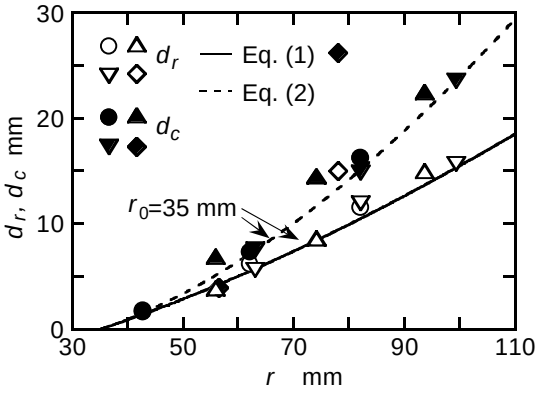

Fig. 5 Output signal of perforation sensor

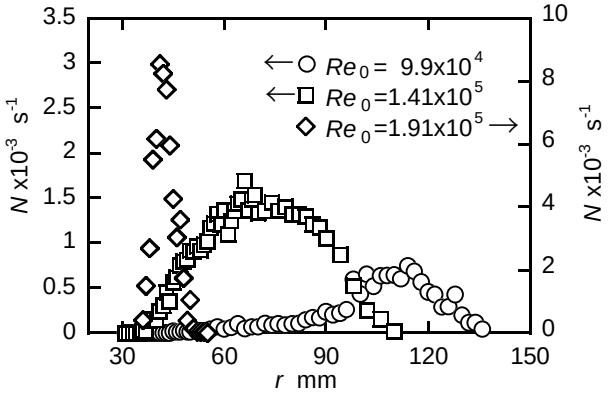

Fig. 6 Number of perforation passage

respectively. Solid and broken lines indicate Eqs. (1) and (2), respectively, and they are calculated under the assumption that perforations occur at r=35 mm. Experimental data are in good agreement with Eqs. (1) and (2). Hence, Eqs. (1) and (2) are useful for representing the growth of perforation.

3.3 Radial distribution of perforations

The passages of perforations at a series of downstream positions were detected using the electric perforation sensor. Figure 6 shows the number of perforation passing through each radial position per unit time, N. When Re_0=9.9x10^4, N increases abruptly at a range of r=95 to 110 mm. This is because a large number of new perforations appears owing to the thinning of the liquid sheet based on the growth of the flag wave, as shown in Fig. 2(a). On the other hand, when Re_0=1.41x10^5, N begins to increase at r=35 mm, where the laminar-turbulent transition occurs, further increases with r in the ripple wave region, and then decreases beyond r=70 mm. This decrease in N is due to the coalescence of perforations, as shown by arrows 'a' and 'b' in Figs. 4. When Re_0=1.91x10^5, a very large number of perforations occurs at the transition region, and the liquid sheet breaks up quickly.

The void fraction f, i.e. the time fraction that a reference point is within passing perforations, measured using the perforation sensor, is shown by circles in graphs of upper side of Figs. 9. It is found that, since f=100 % means the exhaustive disintegration of the liquid sheet, the disintegration point moves upstream with increasing Re_0 and finally it approaches to the transition point.

4. Stochastic treatment of perforation phenomenon

We assume the existence of a function of position in the liquid sheet and time, $g(r, q, t)$, which specifies the rate of occurrence of perforation per unit area. Each perforation so produced must be followed in its subsequent history. These perforations expand and coalesce as they travel downstream. Thus, if the void fraction, $f(r, q)$, that a given point $P(r, q)$ is within any perforation (void) is to be computed, we must add up the times that $P(r, q)$ is covered with perforations originating upstream somewhere. In this summation, however, we must not count twice those portions of perforations which coalesce.

To do this, consider a (r, q, t) space, Fig.7, where r, q are coordinates on the liquid sheet and t is the time. A source at P_0 produces a perforation that moves and expands downstream. In the (r, q, t) space, the perforation sweeps out a volume of a shape dependent upon the manner and rate of perforation movement and growth. Since the perforation is swept away by the stream

and expands relative to the liquid, the volume will always diverge from P_0 in a cone-like manner. We shall call this the "propagation cone" for a source at $P_0(r_0, q_0, t_0)$. Its surface elements are propagation rays of the perforation (the rays is not straight).

We consider the void fraction that a given point $P(r, q, t)$ is within perforation. P will be in perforation if a source has occurred upstream ($r_0<r$) at such a time that P lies in the propagation cone from P_0. The locus of all points P_0 which can put the point P in perforations is a volume upstream of P as shown in Fig. 8. This volume is also cone-like and has generators that are propagation rays drawn upstream from P. This will be called "the dependence volume" R for P. If there is only one source, then P is in a perforation (void) if that source is in R; otherwise, P is in the liquid. Thus, the probability that P is in perforation due to a source at P_0 is

$$f(P,P_0)=\begin{cases} 1 & \text{if } P_0 \text{ is in } R \\ 0 & \text{if } P_0 \text{ is not in } R \end{cases} \tag{3}$$

In a volume element dV_0 ($=dr_0dq_0dt_0$) at point P_0, there will be $g(P_0)dV_0$ sources, each of which will cause P to be in perforation with probability $f(P, P_0)$. We cannot find the void fraction $f(P)$ that P is in perforation by integrating $f(P, P_0)g(P_0)dV_0$, however, since there may be more than one source in R and the resultant perforation at P would thus be counted twice. To avoid these overlaps, we shall assume that the perforation produced nearest the disk edge will be counted as causing to the perforation in the perforation overlap region.

Let $y(P, P_0)dV_0$ be probability that P is in perforation because of sources in dV_0 at P_0 but not because of any source at $P_0^1(r_0^1, q_0^1, t_0^1)$ with $r_0^1<r_0$, i.e., the source at P_0 is to be counted only if it is the point nearest the disk edge that is affecting P. The probability $y(P, P_0)dV_0$ is connected with $g(P_0)$ by

$$y\,(P,P_0)dV_0 = f(P,P_0)g(P_0)dV_0\left\{1-\int_{R^1} y\,(P,P_0^{\,1})dV_0^{\,1}\right\} \tag{4}$$

where R^1 is the portion of the influence volume R for P which lies between the disk edge $r=r_e$ and the circular plane $r=r_0$. The factor

$$\left\{1-\int_{R_1} y\,(P,P_0^{\,1})dV_0^{\,1}\right\}$$

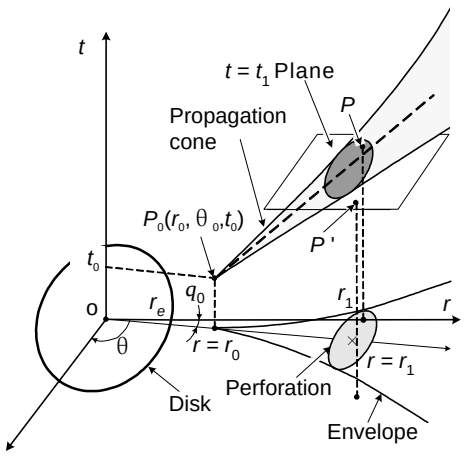

Fig. 7 Propagation of perforation

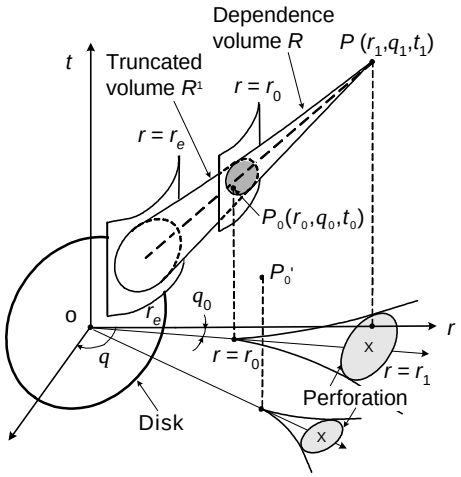

Fig. 8 Dependence volume

is the fraction of the time that P is in liquid so far as sources ahead of r_0 are concerned and, hence, is the fraction of the time during which a source in dV_0 might be effective to put P in perforation. Eq.(4) is to be regarded as an integral equation for $y(P, P_0)$.
After $y(P, P_0)$ is found, the probability that P is in perforation, i.e. the void fraction $f(P)$ during which P is in perforation, is

$$f(P) = \int_R y(P, P_0)\, dV_0 \tag{5}$$

Thus, the relation between the void fraction f and the rate of occurrence of perforation g is expressed by

$$f(P) = 1 - e^{-\int_R g(P_0)\, dV_0} \tag{6}$$

5. Discussions

In this section, using Eq. (6) and the measured void fraction $f(r)$ shown in Figs. 9, we estimate the radial distribution of the rate of occurrence of perforation $g(r)$. To do this, we assume that the occurrence of new perforation is induced by the local thinning of liquid sheet. Observing Figs. 2 and 3 from such a viewpoint, we find out four kinds of causations of the thinning; they are (1) radial spreading of base flow, (2) growth of the flag wave motion, (3) growth of ripple wave and (4) micro-granular wave induced by lamina-turbulent transition.
Furthermore, we divide the liquid sheet into four regions in the downstream direction; (i) laminar flow before the transition, (ii) turbulent flow covered with micro-granular wave, (iii) disturbed flow covered with ripple wave and/or flag wave motion and (iv) liquid droplet flying after complete disintegration of liquid sheet. Then, we assume $g(r)$ for each flow region as follows;

$$g(r) = \begin{cases} 0 & r_e \le r < r_t \quad \text{(i)} \\ a & r_t \le r \le b \quad \text{(ii)} \\ cr(r-b)^n & r < r \le r_d \quad \text{(iii)} \\ 0 & r > r_d \quad \text{(iv)} \end{cases} \tag{7}$$

where a, b and c are constant to be decided, and r_e, r_t and r_d are radii of the disk edge, the transition and the complete disintegration, respectively. In the flow region (iii), we assume fearlessly that the degree of contribution of the radial thinning to g is proportional r and that of growth of flag wave and ripple wave does $(r\text{-}b)^n$.
Using r_t = 34 mm and r_d where f=100 % in Figs. 9 (r_t and r_d are experimental values), we determined the constants a, b and c in Eq. (7) using a method of least squares that fits f on its experimental results with regression equation (6) for both n=1 and 2. In the calculation, dV_0 in Eq. (6) are expressed as follows. The elliptic cross-sectional area of the dependence volume and the circular plane at r=r_0 in Fig. 8 is obtained using the radial length of perforation, d_r, the travelling speed, U_u, the angle made (at the disk center) by two extreme positions of center of perforation detectable at r, $d_c/(r^2+(d_c/2)^2)^{1/2}$, where d_c is the circumferential length of perforation, and r, thus, dV_0 is

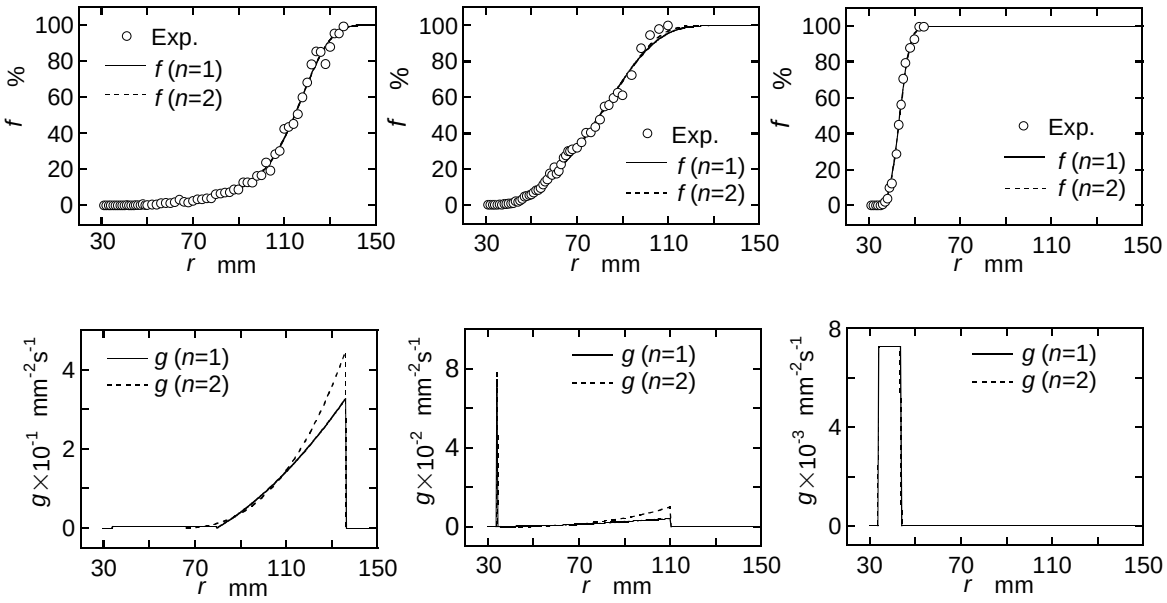

(a) Re_0=9.9x10^4 (b) Re_0=1.41x10^5 (c) Re_0=1.92x10^5

Fig. 9 Void fraction f and rate of occurrence of perforation per unit area g

$$dV_0 = \frac{p d_r(r) d_c(r)}{4} \frac{1}{U_u} \frac{r}{\sqrt{r^2 + \{d_c(r)/2\}^2}} dr$$

The calculated radial distribution of the rate of occurrence of perforation per unit area, $g(r)$, as well as the degree of the fitness of f on experimental result are shown in Figs.9. It is noticed that evident difference between g's values for n=1 and 2 at large radius in Fig. 9(a) gives little effect on f. This is because of the small dependence volume (see Fig. 8) in Eq. (6). The change in g with Re_0 in Figs. 9 clearly shows that although perforation occurs owing to the radial thinning and flag wave amplification at relatively low Re_0, it does owing to the intense turbulence just after the transition at extremely high Re_0. In particular, Fig. 9(c) suggests that the more than ten million of perforations per second are newly produced in a circular area ranging from r=34 to 44 mm and the transition is effective to the atomization of liquid sheet.

References

[1] Hagerty W W and Shea J F 1955 *ASME J Appl. Mech* **22** 509-514
[2] Weihs D 1978 *J. Fluid Mech* **87** 289-298
[3] Mansour A and Chigier N 1989 *Phys. Fluids A* **2** 706-719
[4] Mccreery G E and Stoots C M 1996 *Int. J. Multiphase Flow* **22** 431-452
[5] Dombrowski N and Fraser R P 1954 *Phil. Trans. Royal Soc. Lond* **18** 203-213
[6] Spielbauer T M and Aidun C K 1994 *ASME J. Fluids Eng* **116** 728-734
[7] Azuma T and Hoshino T 1984 *Bull. JSME* **27** 2739-2780
[8] Azuma T 1998 *JSME Int.Journal B* **41** 493-501
[9] Azuma T, Morishima N and Nakayabu Y 1987 *Trans. JSME* **53** 2007-2014(in Japanese)
[10] Azuma T and Morishima N 1987 *Trans. JSME* **53** 2348-2355(in Japanese)
[11] Azuma T and Morishima N 1988 *Trans. JSME* **54** 361-366(in Japanese)
[12] Wakimoto T and Azuma T 1999 *JSME Int. Journal B* **42** 214-223
[13] Watson E J 1964 *J. Fluid Mech* **20** 481-499
[14] Fraser R P, Eisenklam P, Dombrowski N and Hasson D 1962 *AIChE Journal* **8** 672-680